Origin and abundances of volatiles on Mars from the zinc isotopic composition of Martian meteorites

Marine Paquet, Paolo A Sossi, Frédéric Moynier

Origin and abundances of volatiles on Mars from the zinc isotopic composition of Martian meteorites

M. Paquet[1]*, Paolo A. Sossi[2], Frédéric Moynier[1]

[1]Université Paris Cité, Institut de Physique du Globe de Paris, CNRS, 1 rue Jussieu 75005 Paris
[2]Institute of Geochemistry and Petrology, ETH Zürich, Clausiusstrasse 25 CH-8092 Zürich
(*corresponding author: paquet@ipgp.fr, moynier@ipgp.fr)

Total Word Count: 5296 words

References: 95

Keywords: Mars, zinc isotopes, volatile elements, meteorites, chondrites

Abstract (218 words)

Volatile elements are key to understanding the accretion and differentiation processes that formed the terrestrial planets. Relative to the solar photosphere or carbonaceous Ivuna-type (CI) chondrites, the terrestrial planets are depleted in moderately volatile elements (MVEs), with the Earth being more depleted in MVEs than Mars. Mass-dependent and mass-independent stable isotope variations of MVEs, such as Zn, can be used to determine the origin of volatile depletion on Mars. Here we present Zn isotopic compositions of ten Martian meteorites, spanning the major petrologic groups, and show that the Zn isotope composition of the Martian mantle, representative of the Bulk Silicate Mars (BSM), has a δ^{66}Zn (per mille deviation of the ^{66}Zn/^{64}Zn from the JMC-Lyon standard) of +0.50 ± 0.18. This is distinctly heavier than that of the Earth (+0.16 ± 0.06 ‰). The BSM Zn isotope composition could partly reflect fractionation during volatile loss by evaporation consistent with the isotopic composition of other volatile elements (e.g., K). The mass-independent Zn isotopic composition of Mars, ε^{66}Zn (per 10,000 deviation of the ^{66}Zn/^{64}Zn from the terrestrial standard JMC-Lyon, normalized to ^{68}Zn/^{64}Zn) is intermediate between carbonaceous chondrites (CC) and non-carbonaceous chondrites (NC), but with stronger affinity to the NC compared to that of the Earth. Therefore, planets further from the Sun are not necessarily made from a higher fraction of CC-like material.

1. Introduction

Barring a sample return mission to Mars, Martian meteorites are the sole tangible records of its crust available for laboratory investigation. These samples provide insights into the composition of Mars, as well as the processes that led to its accretion and differentiation (e.g., McSween, 1994; Nyquist et al., 2001; Treiman et al., 2000; Halliday et al., 2001; McSween et al., 2009; Taylor, 2013; Tait and Day, 2018; Udry et al., 2020; Paquet et al., 2021; Tian et al., 2021). Volatile elements play an essential role in the evolution of planetary bodies. However, the timing, budget, nature and extent of volatile-depletion in planetary bodies during the earliest stages of solar system evolution remain poorly constrained. The terrestrial planets are depleted in moderately volatile elements (MVEs) relative to the Sun or CI-chondrites, (e.g., Anders and Owen, 1977; Dreibus and Wänke, 1987; Palme and O'Neill, 2014; Khan et al., 2022). Recent work on K isotopes showed that Martian meteorites have systematically heavier K isotopic compositions than the Bulk Silicate Earth (BSE), suggesting that volatile depletion proceeded to a greater extent, producing stronger K isotope fractionation by evaporation relative to their potential precursor materials (Tian et al., 2021). However, this interpretation contrasts with the observation that the abundances of volatile elements, such as Zn, Rb and K, are higher in the estimated composition of the Martian mantle than in the BSE (Yoshizaki and McDonough, 2020; Khan et al, 2022).

Zinc is an ideal element to investigate volatile delivery and loss during planetary accretion (Day and Moynier, 2014) because it is lithophile and moderately volatile (with a half-condensation temperature (T_c) of 704 K), more so than K (T_c = 993 K) under solar nebula conditions (Wood et al., 2019). Wood et al. (2014) showed Zn also exhibits chalcophile behavior to some extent, resulting in Zn partitioning into metal slightly increasing with the S content in the metal. Recent

studies suggested that the Martian core may be richer in S than that of the Earth, with ~10 wt.% of S (e.g., Wang et al., 2016; Steenstra and van Westrenen, 2018; Yoshizaki and McDonough, 2020; Khan et al. 2022). For 10 wt.% of S in the metal, the partition coefficient for Zn is $0.06 \times D_{Fe}$ (Wood et al., 2014), or $D_{Zn} \sim 0.06$ for $D_{Fe} \sim 10$ (Righter and Drake, 1999) – value that decreases with increasing pressure (Mann et al., 2009). Limited to negligible Zn isotope fractionation is expected due to metal-silicate and sulfide-silicate partitioning (Bridgestock et al., 2014; Mahan et al., 2017; Xia et al. 2019) with respect to the temperatures required for the formation of the Martian core (~2300 K; e.g., Righter and Drake, 1996; Rai and van Westrenen, 2013), independently of the S content of the experiments. Thus, it is reasonable to assume that the Bulk Mars and the Bulk Silicate Mars have nearly identical Zn isotopic composition. Furthermore, Zn exhibits limited isotope fractionation (<0.1 ‰ per atomic mass unit) during igneous processes on Earth, namely partial melting and fractional crystallization (e.g., Chen et al., 2013; Sossi et al., 2018). In terrestrial and chondritic samples, variations of $\delta^{66}Zn$ (the per mille deviation of the $^{66}Zn/^{64}Zn$ ratio from the JMC-Lyon standard) larger than 1‰ have been observed mostly in association with volatility-related processes (e.g., Moynier et al., 2006, 2009, 2011; Kamber and Schoenberg, 2020; Mathur et al., 2021). Thus, Zn isotopic fractionation, combined with variations in Zn abundances in igneous rocks from various differentiated planetary bodies, such as the Earth, the Moon or Mars, can reveal significant differences in volatile depletion and recondensation events for these bodies.

Previous Zn isotopic data for Martian meteorites show a range of $\delta^{66}Zn$ from +0.13 to +0.35‰, defining a mean value (+0.25 ± 0.11 ‰, 2SD n=11; Paniello et al., 2012) that is not resolvable from the isotopic composition of the BSE (+0.16 ± 0.06 ‰ to +0.20 ± 0.03 ‰; McCoy-West et al., 2018; Sossi et al., 2018; Doucet et al., 2020; Fang et al. 2022) within error. Thus, it is

78 necessary to re-evaluate the Zn isotopic composition of Mars, to test whether the hypothesis that
79 volatile depletion and associated isotopic fractionation should be more pronounced on smaller
80 bodies, based on K isotopes (Tian et al., 2021), also holds for Zn. To better estimate the Zn isotopic
81 composition of the Bulk Silicate Mars (BSM), we present new high precision Zn isotope data for
82 ten Martian meteorites that represent the major petrologic types. Combined with previous
83 measurements, this new dataset allows assessment of the Zn isotope composition of the Martian
84 mantle. After accounting for the effects of shallow-level crystallization and partial melting, it is
85 possible to derive a δ^{66}Zn value for the BSM. We interpret these data in terms of the accretion-
86 and differentiation history of Mars.
87
88 In addition, nucleosynthetic anomalies provide essential information to identify the origin
89 of the material accreted to planetary bodies, as well as early Solar System conditions and processes
90 (e.g., Clayton and Mayeda, 1996; Trinquier et al., 2007, 2009; Burkhardt et al., 2021; Savage et
91 al., 2022; Steller et al., 2022; Martins et al., 2023). Zinc isotopic anomalies, defined as ε^{66}Zn
92 (deviation in parts per 10,000 of the ^{66}Zn/^{64}Zn from the terrestrial standard JMC-Lyon, normalized
93 to ^{68}Zn/^{64}Zn), exhibit a difference between non-carbonaceous chondrite (NC) and carbonaceous
94 chondrite (CC) material (Savage et al. 2022; Steller et al. 2022; Paquet et al., 2022), as also
95 observed in more refractory elements (Trinquier et al., 2007, 2009; Budde et al., 2016; Kruijer et
96 al., 2017; Nanne et al., 2019). The recognition that these meteorite groups define two distinct
97 isotopic populations permits the origin of volatile elements on Earth to be quantified, because
98 Earth has a mass-independent Zn isotopic composition intermediate between CC and NC material
99 (Savage et al., 2022; Steller et al., 2022; Paquet et al., 2022). Such modeling based on Zn
100 nucleosynthetic anomalies indicates that ~30% of Earth's Zn budget originates from carbonaceous

chondrites, which can be explained by the accretion of ~5 to 12% by mass of CI/Ryugu-like or CV-like material, respectively (Savage et al., 2022; Steller et al., 2022; Paquet et al., 2022), with the remainder coming from NC material. Because the different elements used to define the NC-CC dichotomy record different stages of a planet's accretion history owing to their different siderophilicities and volatilities (e.g., Dauphas, 2017), the information contained in Zn anomalies differs from that in other elements. Following the same approach, we use the mass-independent Zn isotopic composition of Mars to better understand the provenance of volatile elements on Mars.

2. Samples and methods

2.1 Petrological characteristics

Martian meteorites are the only samples currently available from Mars and are traditionally divided into three main groups: shergottites, nakhlites and chassignites, collectively termed SNCs. They are igneous rocks and have mafic to ultramafic compositions (~4 to 30 wt.% MgO; e.g., Udry et al., 2020 and references therein). Shergottites, broadly basaltic rocks derived from partial melting of distinct regions of the Martian mantle, are the most abundant class of Martian meteorites (~89% of the total collection by number; Udry et al., 2020). Shergottites are usually divided into three petrographically defined groups (basaltic, olivine-phyric and poikilitic [ultramafic cumulates]) but also into three geochemical groups based on their incompatible trace element abundances and lithophile isotope ratios (enriched, intermediate and depleted; Borg and Draper, 2003). Nakhlites and chassignites are cumulates: nakhlites are clinopyroxenites to olivine-clinopyroxenites that comprise cumulus olivine and pyroxene with minor glass, plagioclase, phosphate minerals, fayalite-rich olivine in the mesostasis, titanomagnetite, and sulfides, whereas chassignites are dunites and contain cumulus olivine with chromite inclusions and interstitial plagioclase, orthopyroxene, phosphate and sulfide minerals (e.g., Treiman, 2005; Udry et al.,

2020). Nakhlites and chassignites have similar crystallization (~1.3 Ga) and ejection (~11 Ma) ages, which suggests that they likely originate from the same location on Mars (Nyquist et al., 2001; Cohen et al., 2017; Udry and Day, 2018).

2.2 Zinc purification and measurements

Zinc isotopic compositions were measured in ten Martian meteorites, including seven shergottites (depleted: Allan Hills [ALHA] 77005, Dar al Gani [DaG] 476, Elephant Moraine [EETA] 79001, Tissint; enriched: Larkman Nunatak [LAR] 06319, Roberts Massif [RBT] 04262, Zagami), two nakhlites (Miller Range [MIL] 0346, MIL090032) and one orthopyroxenite (ALH 84001).

For each sample, ~100 mg of homogenized powder was dissolved using a mixture of concentrated HNO_3/HF and heated at 130°C in PTFE beakers. Following evaporation of the HNO_3/HF, samples were subsequently treated with 6 $mol.L^{-1}$ HCl and heated again to dissolve remaining fluoride complexes. Samples were then evaporated to dryness. Chemical purification was conducted for some samples at the Institut de Physique du Globe de Paris and for others at the Australian National University, Canberra. In Paris, the analytical methodology followed that described by van Kooten and Moynier (2019), while in Canberra it followed the procedure described in Sossi et al. (2015). The Zn isotope compositions were then measured using a Thermo Scientific Neptune Plus Multi-Collector Inductively-Coupled-Plasma Mass Spectrometer (MC-ICP-MS) at either IPGP or at ANU, following the methods described in van Kooten and Moynier (2019) and Sossi et al. (2015), respectively.

Zinc isotope compositions are reported in **Table 1**, as the deviation in parts per 1000 from the terrestrial standard JMC-Lyon:

$$\delta^{x}Zn = \left[\frac{\left(\frac{^{x}Zn}{^{64}Zn}\right)_{Sample}}{\left(\frac{^{x}Zn}{^{64}Zn}\right)_{JMC-Lyon}} - 1\right] \times 10^{3} \quad (1)$$

where x=66 or 68. Uncertainties are given as the 2 times standard deviation (2SD) of replicate measurements. Standard reference powders were analyzed together with the SNCs, yielding values of $\delta^{66}Zn$ = ±0.29 ± 0.01 (2SE, n=4; IPGP) and +0.28 ± 0.03 (2SE, n=2; ANU) for BHVO-2 and +0.21 ± 0.04 (2SE, n=2; ANU) for Allende, respectively, which are consistent with recommended literature values (Moynier et al., 2017). The external reproducibility was therefore better than 0.04 on the $\delta^{66}Zn$ value.

Zinc isotope measurements were also corrected for mass-dependent fractionation using the exponential law (Russel et al., 1978), with the internal normalizing ratio of $^{68}Zn/^{64}Zn$ of 0.3856 (Rosman, 1972). Zinc isotopic anomalies represent the deviation from the mass-dependent fractionation line (**Figure S1**) and are quantified using the epsilon notation, which corresponds to the deviation in parts per 10,000 from the terrestrial standard JMC-Lyon, as follows:

$$\varepsilon^{66}Zn_{C} = \left[\frac{\left(\frac{^{66}Zn}{^{64}Zn}\right)_{Sample}}{\left(\frac{^{66}Zn}{^{64}Zn}\right)_{JMC-Lyon}} - 1\right] \times 10^{4} \quad (2)$$

where c is the normalizing ratio $^{68}Zn/^{64}Zn$.

3. Results

All Martian meteorites fall slightly above the mass-dependent fractionation line in a $\delta^{68}Zn$ versus $\delta^{66}Zn$ plot (**Figure S1**), which is consistent with previous studies on Mars (e.g., Paniello et

al., 2012). Martian meteorites span a range of δ^{66}Zn from +0.18 ± 0.02 (Tissint) to +0.52 ± 0.02 (ALHA 77005), with an average value of +0.36 ± 0.08 (**Figure 1, Table 1**). Five of the Martian meteorites analyzed in Paniello et al. (2012) are also presented herein **(Figure 2)**. It is worth noting that data from this study tend to exhibit slightly higher δ^{66}Zn values than those from Paniello et al. (2012), which could be attributed to heterogeneities in the measured Martian meteorites.

Nakhlites, enriched and depleted shergottites are, on average, indistinguishable within uncertainty (+0.36 ± 0.00 ‰ [n=2, 2SE], +0.36 ± 0.07 ‰ [n=3, 2SE] and +0.35 ± 0.12 ‰ [n=4, 2SE], respectively). This assertion is confirmed by a two-sample Kolmogorov-Smirnov test that returned D values of 0.29 (depleted vs. enriched shergottites), 0.71 (depleted shergottites vs. nakhlites) and 0.71 (enriched shergottites vs. nakhlites), where D is the maximum absolute value of the difference between the cumulative distribution functions for the different groups of Martian meteorites (Miller and Miller, 2018). For a confidence level of $\alpha = 0.05$, the D values need to be greater than $D_{criteria} = \sqrt{-l\,n(\alpha/2)\,/2} \times \sqrt{(n_1 + n_2)/n_1/n_2} = 0.67$, where n_1 and n_2 are the numbers of samples in each population.

The Martian samples with the lowest δ^{66}Zn values tend to exhibit lower MgO contents **(Figure 2a)**, opposite to what is observed for terrestrial basalts (Sossi et al., 2018), however there is no correlation with their Zn abundances **(Figure 2b)**. Our study also provides evidence for the first mass-independent Zn isotope variations (ε^{66}Zn) in Martian meteorites (**Figure 4**), ranging from -0.25 to +0.07, except for one MIL 03346 replicate (+0.42) (**Table 1**), with an average value for Mars of -0.07 ± 0.08 (2SE, n = 10).

4. Discussion

As demonstrated above, Martian meteorites exhibit a range of δ^{66}Zn values. These variations may arise from terrestrial late-stage and alteration processes, magmatic differentiation, volatile depletion processes prior or during accretion, and core formation on Mars. In the following discussion, we will address the potential contribution of these different processes to the Zn isotopic compositions of the Martian meteorites individually.

4.1 Potential disturbance of Zn during late-stage processes

All Martian meteorites considered in this study were recovered from hot (Sahara) or cold (Antarctica) deserts, and therefore may have undergone terrestrial alteration and weathering, potentially perturbing the Zn isotope compositions in these rocks from their primary igneous values. Such alteration processes can affect refractory lithophile isotope compositions by the formation of secondary minerals in hot desert environments (e.g., Crozaz et al., 2003; Symes et al., 2008), or remobilized lanthanides, mostly in the presence of phosphates, due to prolonged ice exposure in cold desert environments (e.g., Crozaz et al., 2003). Even though isotopic disturbances have been observed in Antarctic and hot desert meteorites, initial $^{87}Sr/^{86}Sr$ ratios for most samples investigated here show little variation relative to the 4.5 Ga line (e.g., Tait and Day, 2018), supporting the hypothesis that these Martian meteorites underwent limited terrestrial alteration. In terrestrial rocks, Zn is mostly hosted in silicates (olivine, orthopyroxene) and oxides (ilmenite, spinel) (e.g., Le Roux et al., 2011; Fang et al., 2022), and is mobile only when the minerals are heavily altered (Debret et al. 2021), which is not the case here. Moreover, normalizing Zn abundances to another element, such as Fe, that behaves similarly during petrogenetic processes, provided it is predominantly ferrous (e.g., Le Roux et al., 2010; Davis et al., 2013), represents a test of the degree to which the original magmatic abundances of Zn are preserved. Thus, if

undisturbed, Martian meteorites owing to the relatively reduced fO_2 (~IW; Wadhwa, 2001) under which they crystallized, should lie on olivine- and/or pyroxene control lines producing near constant Zn/Fe ratios. Samples that experienced secondary weathering/alteration should then diverge from the constant Zn/Fe value. All Martian meteorites have comparable Zn/Fe ratios, ranging between 2.6×10^{-4} and 5.1×10^{-4}, even though they are not representative of a single differentiation suite, with the exception of ALH 84001 which plots off the array (7.3×10^{-4}, **Table 1**). ALH 84001 is an orthopyroxenite that preserves evidence of interaction with aqueous fluids while on Mars in the form of microscopic carbonate disks (Thomas-Keprta et al., 2009). Despite this, its δ^{66}Zn is $+0.31 \pm 0.01$ and is consistent with the other Martian samples. Thus, the Zn isotope composition of the Martian meteorites can be regarded as reflecting the primary signature of magma from which they derived.

4.2 Zinc fractionation during magmatic processes

Magmatic processes such as partial melting and fractional crystallization have been shown to fractionate Zn isotopes in terrestrial environments (e.g., McCoy-West et al. 2018). Strikingly, the array defined by Martian magmas in MgO - δ^{66}Zn space is a mirror image of that expressed in terrestrial basalts or komatiites (e.g., Chen et al., 2013; Sossi et al., 2018), with decreasing δ^{66}Zn with decreasing MgO **(Figure 2a)**. This behavior was also noted by Paniello et al. (2012), but the precision of Zn isotopic data was not sufficient to define a trend.

Mineral proportions in shergottites are similar to those in terrestrial basalts, with olivine constituting 7 – 29 % of olivine-phyric shergottites and 35 – 60 % of poikilitic shergottites (Bridges and Warren, 2006; Sarbadhikari et al., 2009). The bulk of the remainder of the minerals is comprised of pyroxenes (largely pigeonite), in which Mg^{2+} and Fe^{2+} are also octahedrally

coordinated (Cameron et al., 1973). Therefore, as in terrestrial basalts, the Zn budget of the solid phases is dominated by ferromagnesian silicates. Since $^{VI}Zn^{2+}$ is the prevailing bonding environment owing to its substitution for $^{VI}Fe^{2+}$ in these phases, hypotheses for differences in the terrestrial and Martian arrays must appeal to changes in melt composition.

In natural terrestrial silicate melts, Zn is expected to occur in tetrahedral coordination, owing to its lack of octahedral site preference energy, and by analogy with Zn-bearing minerals and in aluminosilicate glasses (e.g., Neumann, 1949; Dumas and Petiau, 1986). However, the distinctive feature of Martian magmas is their high FeO_t contents, which acts predominantly as a network modifier, as Fe is almost exclusively Fe^{2+} (Righter et al., 2013). For primary Martian magmas, such as EETA 79001A (Filiberto and Dasgupta, 2011), NBO/T is ~ 2, which is higher than typical terrestrial magmas (up to ~1), but similar to komatiites. Increasing proportions of network modifiers tend to increase the coordination number, such that a higher proportion of Zn would be expected to be in VI-fold coordination in such melts. This behavior is corroborated by the tendency for other divalent first-row transition metals, such as Co and Ni, to exist in octahedral complexes in more basic compositions (e.g., Farges et al., 2001). However, while this shift will reduce isotopic fractionation between the two phases, the melt becoming enriched in heavy isotopes in terrestrial melts (Sossi et al., 2018), it is unknown whether it would reverse the trend to the extent observed for Martian magmas.

Since shergottites and nakhlites/chassignites are likely not cogenetic magmas (Wadhwa, 2001; Borg and Draper, 2003; Bridges and Warren, 2006), their chemical and isotopic signatures could also derive from differences in their source composition. However, given the degree of

263 homogeneity shown for the Zn isotopic composition of terrestrial rocks (e.g., Sossi et al., 2018),
264 this is unlikely. Another possibility is that a fraction of the Zn is hosted in oxides (e.g., spinel), in
265 which it exists in IV-fold co-ordination (O'Neill and Navrotsky, 1983) and should therefore
266 concentrate the heavier isotopes, though this would also be the case on Earth. Volatile loss of Zn
267 during magma emplacement is also precluded (Toutain et al., 2008) because it would result in the
268 preferential loss of the lighter isotopes of Zn, causing δ^{66}Zn to increase towards lower MgO
269 contents, which is the opposite of what is observed for Martian meteorites (**Figure 2**). Additional
270 experiments on Zn isotope fractionation in igneous systems are required to understand the drivers
271 of Zn isotope variations in natural rocks, and in particular the role of its co-ordination environment,
272 both in minerals and melts.
273
274 *4.3 Zinc composition of the Bulk Silicate Mars*
275 The high Fe content of Bulk Silicate Mars as calculated from the SNC suite is consistent
276 with spectral data of the Martian surface, which reveals similarly enriched FeO contents relative
277 to Earth's mantle or its basaltic crust (Taylor et al., 2006; McSween et al., 2009; Khan et al., 2022).
278 This observation is true for other divalent cations, including Mg^{2+} and Mn^{2+}, where Mg/Fe and
279 Mn/Fe ratios of shergottites and in-situ measurements of Martian samples fall on liquid lines of
280 descent (e.g., McSween et al., 2009). Such similarity arises from the near-absence of Fe^{3+} in the
281 Martian mantle (e.g., Righter et al., 2013), and suggests that Zn^{2+} behaves analogously to Fe during
282 magmatic differentiation. Their concordance increases the likelihood that the concentrations, and
283 potentially isotopic compositions of Zn in the SNCs are reflections of that of the Martian mantle.
284 Therefore, although the sample size is small, the SNCs span a broad range of MgO contents that
285 allow for the characterization of trends likely controlled by igneous processes **(Figure 2a)**. The
286 fact that these appear to be preserved also supports closed-system transport of the meteorites to

Earth with respect to Zn. Extrapolation of the shergottite array (with the exception of Tissint which plots within the BSE range) to the MgO content of the Martian mantle of 32.81 ± 0.22 wt.% (Khan et al., 2022) yields a $\delta^{66}Zn = +0.50 \pm 0.18$, distinctly heavier than that of the Earth (from +0.16 ± 0.06 ‰ to +0.20 ± 0.03 ‰; McCoy-West et al., 2018; Sossi et al., 2018; Doucet et al., 2020; Fang et al., 2022). Alternatively, using the average of the shergottites results in a value of +0.38 ± 0.05 ‰ (2SE, n = 6), which lies within uncertainty of our reported estimate based on the $\delta^{66}Zn$ – MgO correlation ($R^2 = 0.65$, excluding Tissint). Thus, for the following discussion we report our initial estimate of +0.50 ± 0.18 ‰ for the BSM.

4.4 Behavior of Zn and other moderately volatile elements during accretion of Mars

In $\delta^{66}Zn$ – Zn/Mg space, the Earth's estimate plots at the intersection of 1) the carbonaceous chondrites trend following the equation $\delta^{66}Zn = 0.363 \log(Zn/Mg) + 1.40$ (Luck et al., 2005; Pringle et al., 2017; Sossi et al., 2018) and 2) the path of fractionation induced by evaporation or condensation, for a fractionation factor between liquid/solid and gas yielding the composition of the Moon (Sossi et al., 2018). The Earth's composition is interpreted as having been derived from the accretion of material that experienced chemical and isotopic fractionation in the solar nebula, similar to that experienced by carbonaceous chondrites but extended to more volatile-depleted extremes. Our estimate of the bulk Zn/Mg ratio of Mars, 3.34×10^{-4} (MgO = 32.81 ± 0.22 wt.%, Zn_{mantle} = 65.9 ± 8.5 ppm), would result in a composition of +0.14 ‰, similar to that of the Earth **(Figure 3)**, were Mars to have also inherited the majority of its Zn from carbonaceous chondrite-like components. However, with an estimated composition of +0.50 ± 0.18 ‰ for the BSM, the $\delta^{66}Zn$ of Mars is greater than that defined by the carbonaceous chondrite array.

Accounting for a similar proportion of the total Zn residing in the Martian core (which corresponds to a mass fraction of 25%, with a higher S content; e.g., Khan et al., 2022) that in the Earth's core (Sossi et al., 2018), we obtain Zn_{bulk} = 99.8 ppm. Assuming that no Mg partitioned into the core (e.g., Ringwood and Hibberson, 1991), the Zn/Mg ratio of Mars is 5.05×10^{-4}. Notably, Zn isotopic fractionation at pressure and temperature conditions relevant for the formation of the Martian core is negligible (Brigestock et al., 2014; Mahan et al., 2017). Thus, it would require [Zn] = 651 ppm for Mars to plot on the carbonaceous chondrite array, corresponding to a partition coefficient of $D_{Zn} \sim 45$, which is not compatible with experimental data (e.g., Wood et al., 2014). Alternatively, we obtain [Zn] = 305 ppm and $D_{Zn} \sim 19$ if we consider a $\delta^{66}Zn$ of +0.38.

However, the average of SNC meteorites indicates that Bulk Silicate Mars exhibits a $\varepsilon^{66}Zn$ value (–0.08 ± 0.07, 2SE, n = 10) intermediate between that of ordinary and carbonaceous chondrites (non-carbonaceous (ordinary + enstatite) chondrites: –0.20 ± 0.04, 2SE, n = 20; carbonaceous chondrites: +0.31 ± 0.05, 2SE, n = 22, and Ryugu asteroid materials: +0.33 ± 0.03, n=4 [Savage et al., 2022; Steller et al., 2022; Paquet et al., 2022]), similar within error to that of the Earth (+0.015 ± 0.075, 2SE [Savage et al., 2022]; –0.07 ± 0.013, 2SE [Steller et al., 2022]), but closer to that of the NC endmember (**Figure 4**). Because there are no known terrestrial processes which can mass-independently fractionate Zn isotopes, the intermediate $\varepsilon^{66}Zn$ of Mars between carbonaceous chondrites and ordinary chondrites suggests a potential mixing between these two reservoirs to explain Mars' isotopic compositions, which is consistent with other nucleosynthetic anomalies such as in Ti, Cr, O, Ca or Fe (e.g., Clayton and Mayeda, 1996; Trinquier et al., 2007, 2009; Schiller et al., 2018, 2020). Moreover, since the mass independent

isotope composition of Zn indicates it was largely inherited from an NC-like reservoir on Mars, rather than from CCs, there is no reason to expect that bulk Mars lies on the CC array, strongly arguing against significant quantities of Zn in the Martian core. Using the $\varepsilon^{66}Zn$ values from Mars, carbonaceous and ordinary chondrites, together with their Zn abundances (see **Table 2** for details), we calculated the proportions of CC and NC required to reproduce Mars' $\varepsilon^{66}Zn$, which yields to the following proportions: 4 % Ryugu-like material + 96 % NC (6 % CI + 94 % NC, or 14 % CV + 86 % NC), representing ~22 % of Mars' Zn delivered by outer solar system material, which is slightly lower than the estimation for the Earth's (~30 %; Savage et al., 2022; Steller et al., 2022; Paquet et al., 2022). This observation contrasts with the notion that planets further from the Sun should have higher contribution from outer Solar System (e.g., Ryugu-like or CC-like) materials.

It is then possible to estimate the $\delta^{66}Zn$ and Zn/Mg of such a mixture (assuming the Mg content of Mars, ~19.8 wt.% [Khan et al., 2022], is not affected by evaporation), and calculate the isotopic fractionation induced by evaporation, assuming a Rayleigh evaporation law and a fractionation factor $\Delta^{66}Zn_{liq\text{-}vap}$. The scenario modeled by Sossi et al. (2018) used $\Delta^{66}Zn_{liq\text{-}vap} = 1‰$ to account for the composition of the Moon derived from the Earth (**Figure 3**). We consider two endmembers: the first in which all the non-carbonaceous chondrites are ordinary chondrites (OC), and the second in which all the non-carbonaceous chondrites are enstatite chondrites (EH). Elemental abundances for OC and EH are from Lodders and Fegley (1998) and average $\delta^{66}Zn$ for OC is from Paniello (2013, PhD thesis Washington University Saint Louis) and Creech and Moynier (2019), and average $\delta^{66}Zn$ for EH is from Moynier et al. (2011), respectively (Table 2). In this scenario, the isotopic fractionation induced by ~20-25 % evaporation (with $\Delta^{66}Zn_{liq\text{-}vap} = 1‰$) from a mixture of 4 % Ryugu-like material (or from 6 % of CI to 14 % of CV) and 96 % OC

(94 % and 86 %, for CI and CV, respectively) reproduces both the Zn mass-dependent and -independent BSM composition (**Figure 3**). Starting compositions calculated from a mixture of outer Solar System material and EH are too enriched in Zn to reproduce the BSM. These values are consistent with previous studies which argued in favor of 9 to 18 % of carbonaceous chondrite-like material based on Cr anomalies and $\Delta^{17}O$ (Warren, 2011), and up to 36 % of CI-like material based on $\mu^{48}Ca$ anomalies (Schiller et al., 2018) to account for Mars' composition.

Assuming that equilibrium isotope fractionation between liquid and vapor prevailed ($\Delta^{66}Zn_{liq-vap} = \frac{(+0.31\times10^6)}{T^2}$, where T is in K; Ducher et al., 2016), then the temperature required to achieve a $^{66}Zn/^{64}Zn$ fractionation factor of 1‰, consistent with the Zn/Mg and $\delta^{66}Zn$ composition of Mars, is constrained between 557 and 704 K. At such low temperatures, it is difficult to engender significant isotope fractionation in the condensed phase during vapor loss from a Mars-mass planet because the temperatures are well below the solidi of the silicate minerals that comprise the Martian mantle, meaning mass transport is not sufficiently rapid to cause global Zn depletion. Therefore, should equilibrium isotope fractionation during evaporation be responsible for its Zn isotopic composition, then this would have had to have occurred on small (e.g., cm-sized) precursor grains from which gas-solid separation is facilitated. Curiously, the temperatures calculated above bracket the 50 % condensation temperature of Zn from the solar nebula at 10^{-4} bar (~700 K; Wood et al. 2019). Equilibrium isotope fractionation factors at higher temperatures are not able to reproduce the combined Zn/Mg ratio and isotopic composition for the BSM by evaporation in a CC-like precursor or during Mars' history (**Figure 5**). A more accurate picture of the Zn isotope composition of Mars is precluded due to the spread of Zn isotope values in OCs, ranging from -1.31 ‰ to + 1.75 ‰ (**Figure 3**). Nevertheless, the general conclusion holds

379 that, should the Zn isotope composition of the BSM have been subsequently modified by
380 equilibrium evaporation, then it must have occurred at low temperatures that could only have
381 existed in the solar nebula. Alternatively, evaporation did not proceed under equilibrium
382 conditions, but was rather kinetic in nature to induce larger isotopic fractionation, with a $\Delta^{66}Zn_{liq\text{-}vap}$ factor ~1 ‰ that reflected the local evaporation environment. It is worth noting that the
384 maximum effect on $\varepsilon^{66}Zn$ expected for a fractionation (kinetic or under equilibrium) of 0.5‰ is
385 ~0.1ε, which is within the error of the estimate of the BSM composition. Because Mars' $\varepsilon^{66}Zn$ is
386 close to that of NC, it is also possible that Mars' isotopic signature is inherited from its precursors
387 (mainly OC) from the solar nebula, obviating the need for the addition of CC material.
388
389 The apparent isotope differences between CC and NC meteorites, which was first identified
390 for O and Cr isotopes (Clayton and Mayeda, 1996; Trinquier et al., 2007), and later with Ti, Ni,
391 Mo and also Zn anomalies (Trinquier et al., 2009; Warren, 2011; Budde et al., 2016; Kruijer et al.,
392 2017; Nanne et al., 2019; Burkhardt et al., 2021; Savage et al., 2022; Steller et al., 2022), has been
393 ascribed to the spatial location at which these meteorite groups formed, separated by a physical
394 barrier that prevented their mixing over their formation timescales, 1 – 4 Myr after CAI (Kruijer
395 et al. 2017). In this model, the CCs are presumed to have formed in the outer Solar System (i.e.,
396 beyond the orbit of Jupiter) while NCs are derived from the inner Solar System. Physical accretion
397 models for the terrestrial planets, in the context of N-body simulations, both in the Grand Tack-
398 (Jacobson and Morbidelli, 2014) and standard models (Wetherill et al. 1994) indicate that planets
399 that formed further from the Sun should, on average, contain higher fractions of outer Solar System
400 materials (e.g., Wetherill, 1994; Cuzzi and Zahnle, 2004; Rubie et al. 2015; Sossi et al. 2022),
401 though the Grand Tack model results in a more random distribution of material in the inner disk

402 from different heliocentric distances than does the standard model. Although Mars has a
403 marginally higher Zn content than the Earth, that the Zn isotope composition of Mars contains a
404 higher fraction of nominally inner Solar System OC-like material than the Earth suggests that the
405 dichotomy of CC- vs. NC-material may not exclusively relate to their location in the protoplanetary
406 disk. In addition, masses and orbits of terrestrial planets, including Mars, are also consistent with
407 pebble accretion onto protoplanets accreted around Mars' orbit and then migrated to their final
408 position while growing (e.g., Johansen et al., 2021); Mars' isotopic composition closer to the NC
409 than is the Earth could indicate an earlier growth termination for Mars (as indicated in its Hf-W
410 age of 9 Myr compared to ~30 Myr for the Earth; Dauphas and Pourmand, 2011; Kleine and
411 Walker 2017). Mars therefore may not have accreted pebbles of CI composition that drifted later
412 towards the inner part of the protoplanetary disk (e.g., Schiller et al., 2018). In future, isotopic data
413 for other volatile systems with more than 3 isotopes, such as Cd or Te, should be acquired to further
414 investigate the volatile accretion history of Mars by combining mass-dependent isotopic
415 fractionation and nucleosynthetic anomalies to better understand the nature and distribution of
416 volatile-bearing material in the early Solar System.
417

418 **5. Conclusions**

419 We measured the Zn isotopic composition of ten Martian meteorites from the main petrologic
420 groups to investigate the origin of volatile depletion on Mars. Extrapolating the shergottite array
421 to a MgO value representative of the Martian mantle, our new dataset allows assessment of its Zn
422 isotope composition, representative of the BSM (bulk silicate Mars) ($\delta^{66}Zn = +0.50 \pm 0.18$), which
423 is shown to be distinctly heavier than that of the Earth. This composition can be extended to that
424 of the Bulk Mars insofar as negligible Zn isotope fractionation is observed between metal and
425 silicate at pressure and temperature conditions relevant for Martian core segregation. The BSM

426 plots above the carbonaceous chondrite array defined in a δ^{66}Zn vs log(Zn/Mg) plot, arguing in
427 favor of isotopic fractionation during volatile loss by evaporation/condensation, or the provenance
428 of Zn from largely OC-like precursors. The mass-dependent and mass-independent Zn isotope
429 compositions of Mars provide new constraints on the origin of volatile elements, suggesting that
430 between ~4 to 6 % of outer Solar System material (Ryugu-like or CI-like, respectively) were
431 delivered to Mars to account for its Zn budget.

432

433 **Acknowledgements**

434 This work was supported by the IPGP analytical platform PARI, Region Ile-de-France SESAME
435 Grants no. 12015908, and DIM ACAV +, the ERC grant agreement No. 101001282 (METAL)
436 (F.M.) the UnivEarthS Labex program (numbers: ANR-10-LABX-0023 and ANR-11-IDEX-
437 0005-02) (F.M.). P.A.S. was supported by an Australian Postgraduate Award and SNSF
438 Ambizione Fellowship #180025. We thank K. Righter of NASA for providing the MWG samples.
439 We thank Herbert Palme and Klaus Mezger for their constructive comments that improved the
440 manuscript, and Editor Rajdeep Dasgupta for efficient editing of the paper. The authors declare no
441 conflicts of interest. All data referred to in this article can be found in the tables or cited references.

442

443

References

Anders, E., & Owen, T. (1977). Mars and Earth: Origin and Abundance of Volatiles: Mars has only 3 percent of Earth's share of volatiles, but got them from the same meteoritic source. *Science*, *198*(4316), 453-465.

Borg, L. E., & Draper, D. S. (2003). A petrogenetic model for the origin and compositional variation of the Martian basaltic meteorites. *Meteoritics & Planetary Science*, *38*(12), 1713-1731.

Bridges, J. C., & Warren, P. H. (2006). The SNC meteorites: basaltic igneous processes on Mars. *Journal of the Geological Society*, *163*(2), 229-251.

Bridgestock, L. J., Williams, H., Rehkämper, M., Larner, F., Giscard, M. D., Hammond, S., ... & Schönbächler, M. (2014). Unlocking the zinc isotope systematics of iron meteorites. *Earth and Planetary Science Letters*, *400*, 153-164.

Budde, G., Burkhardt, C., Brennecka, G. A., Fischer-Gödde, M., Kruijer, T. S., & Kleine, T. (2016). Molybdenum isotopic evidence for the origin of chondrules and a distinct genetic heritage of carbonaceous and non-carbonaceous meteorites. *Earth and Planetary Science Letters*, *454*, 293-303.

Burkhardt, C., Spitzer, F., Morbidelli, A., Budde, G., Render, J. H., Kruijer, T. S., & Kleine, T. (2021). Terrestrial planet formation from lost inner solar system material. *Science advances*, *7*(52), eabj7601.

Cameron, M., Sueno, S., Prewitt, C. T., & Papike, J. J. (1973). High-temperature crystal chemistry of acmite, diopside, hedenbergite jadeite, spodumene and ureyite. *American Mineralogist: Journal of Earth and Planetary Materials*, *58*(7-8), 594-618.

Chen, H., Savage, P. S., Teng, F. Z., Helz, R. T., & Moynier, F. (2013). Zinc isotope fractionation during magmatic differentiation and the isotopic composition of the bulk Earth. *Earth and Planetary Science Letters*, *369*, 34-42.

Clayton, R. N., & Mayeda, T. K. (1996). Oxygen isotope studies of achondrites. *Geochimica et Cosmochimica Acta*, *60*(11), 1999-2017.

Cohen, B. E., Mark, D. F., Cassata, W. S., Lee, M. R., Tomkinson, T., & Smith, C. L. (2017). Taking the pulse of Mars via dating of a plume-fed volcano. *Nature communications*, *8*(1), 1-9.

Creech, J. B., & Moynier, F. (2019). Tin and zinc stable isotope characterisation of chondrites and implications for early Solar System evolution. *Chemical Geology*, *511*, 81-90.

Crozaz, G., Floss, C., & Wadhwa, M. (2003). Chemical alteration and REE mobilization in meteorites from hot and cold deserts. *Geochimica et Cosmochimica Acta*, *67*(24), 4727-4741.

Cuzzi, J. N., & Zahnle, K. J. (2004). Material enhancement in protoplanetary nebulae by particle drift through evaporation fronts. *The Astrophysical Journal*, *614*(1), 490.

Dauphas, N. (2017). The isotopic nature of the Earth's accreting material through time. *Nature*, *541*(7638), 521-524.

Dauphas, N., & Pourmand, A. (2011). Hf–W–Th evidence for rapid growth of Mars and its status as a planetary embryo. *Nature*, *473*(7348), 489-492.

Davis, F. A., Humayun, M., Hirschmann, M. M., & Cooper, R. S. (2013). Experimentally determined mineral/melt partitioning of first-row transition elements (FRTE) during partial melting of peridotite at 3 GPa. *Geochimica et Cosmochimica Acta*, *104*, 232-260.

Day, J. M. D., & Moynier, F. (2014). Evaporative fractionation of volatile stable isotopes and their bearing on the origin of the Moon. *Philosophical Transactions of the Royal Society A: Mathematical, Physical and Engineering Sciences*, *372*(2024), 20130259.

Debret, B., Garrido, C. J., Pons, M. L., Bouilhol, P., Inglis, E., Sánchez-Vizcaíno, V. L., & Williams, H. (2021). Iron and zinc stable isotope evidence for open-system high-pressure dehydration of antigorite serpentinite in subduction zones. *Geochimica et Cosmochimica Acta*, *296*, 210-225.

Doucet, L. S., Laurent, O., Ionov, D. A., Mattielli, N., Debaille, V., & Debouge, W. (2020). Archean lithospheric differentiation: Insights from Fe and Zn isotopes. *Geology*, *48*(10), 1028-1032.

Dreibus, G., & Wänke, H. (1987). Volatiles on Earth and Mars: A comparison. *Icarus*, *71*(2), 225-240.

494 Ducher, M., Blanchard, M., & Balan, E. (2016). Equilibrium zinc isotope fractionation in Zn-bearing
495 minerals from first-principles calculations. *Chemical Geology*, *443*, 87-96.
496 Dumas, T., & Petiau, J. (1986). EXAFS study of titanium and zinc environments during nucleation in a
497 cordierite glass. *Journal of non-crystalline solids*, *81*(1-2), 201-220.
498 Fang, S. B., Huang, J., Zhang, X. C., Ionov, D. A., Zhao, Z. F., & Huang, F. (2022). Zinc isotope
499 fractionation in mantle rocks and minerals, and a revised δ^{66}Zn value for the Bulk Silicate
500 Earth. *Geochimica et Cosmochimica Acta*, *338*, 79-92.
501 Farges, F., Brown Jr, G. E., Petit, P. E., & Munoz, M. (2001). Transition elements in water-bearing silicate
502 glasses/melts. Part I. A high-resolution and anharmonic analysis of Ni coordination environments
503 in crystals, glasses, and melts. *Geochimica et Cosmochimica Acta*, *65*(10), 1665-1678.
504 Filiberto, J., & Dasgupta, R. (2011). Fe^{2+}–Mg partitioning between olivine and basaltic melts: Applications
505 to genesis of olivine-phyric shergottites and conditions of melting in the Martian interior. *Earth*
506 *and Planetary Science Letters*, *304*(3-4), 527-537.
507 Halliday, A. N., Wänke, H., Birck, J. L., & Clayton, R. N. (2001). The accretion, composition and early
508 differentiation of Mars. *Space Science Reviews*, *96*(1), 197-230.
509 Jacobson, S. A., & Morbidelli, A. (2014). Lunar and terrestrial planet formation in the Grand Tack
510 scenario. *Philosophical Transactions of the Royal Society A: Mathematical, Physical and*
511 *Engineering Sciences*, *372*(2024), 20130174.
512 Johansen, A., Ronnet, T., Bizzarro, M., Schiller, M., Lambrechts, M., Nordlund, Å., & Lammer, H. (2021).
513 A pebble accretion model for the formation of the terrestrial planets in the Solar System. *Science*
514 *Advances*, *7*(8), eabc0444.
515 Kamber, B. S., & Schoenberg, R. (2020). Evaporative loss of moderately volatile metals from the
516 superheated 1849 Ma Sudbury impact melt sheet inferred from stable Zn isotopes. *Earth and*
517 *Planetary Science Letters*, *544*, 116356.
518 Khan, A., Sossi, P. A., Liebske, C., Rivoldini, A., & Giardini, D. (2022). Geophysical and cosmochemical
519 evidence for a volatile-rich Mars. *Earth and Planetary Science Letters*, *578*, 117330.
520 Kleine, T., & Walker, R. J. (2017). Tungsten isotopes in planets. *Annual review of earth and planetary*
521 *sciences*, *45*, 389-417.
522 Kruijer, T. S., Burkhardt, C., Budde, G., & Kleine, T. (2017). Age of Jupiter inferred from the distinct
523 genetics and formation times of meteorites. *Proceedings of the National Academy of*
524 *Sciences*, *114*(26), 6712-6716.
525 Le Roux, V., Dasgupta, R., & Lee, C. T. (2011). Mineralogical heterogeneities in the Earth's mantle:
526 Constraints from Mn, Co, Ni and Zn partitioning during partial melting. *Earth and Planetary*
527 *Science Letters*, *307*(3-4), 395-408.
528 Le Roux, V., Lee, C. T., & Turner, S. J. (2010). Zn/Fe systematics in mafic and ultramafic systems:
529 Implications for detecting major element heterogeneities in the Earth's mantle. *Geochimica et*
530 *Cosmochimica Acta*, *74*(9), 2779-2796.Lodders, K., & Fegley, B. (1998). *The planetary scientist's*
531 *companion*. Oxford University Press.
532 Luck, J. M., Othman, D. B., & Albarède, F. (2005). Zn and Cu isotopic variations in chondrites and iron
533 meteorites: early solar nebula reservoirs and parent-body processes. *Geochimica et Cosmochimica*
534 *Acta*, *69*(22), 5351-5363.
535 Mahan, B., Moynier, F., Beck, P., Pringle, E. A., & Siebert, J. (2018). A history of violence: Insights into
536 post-accretionary heating in carbonaceous chondrites from volatile element abundances, Zn
537 isotopes and water contents. *Geochimica et Cosmochimica Acta*, *220*, 19-35.
538 Mahan, B., Siebert, J., Pringle, E. A., & Moynier, F. (2017). Elemental partitioning and isotopic
539 fractionation of Zn between metal and silicate and geochemical estimation of the S content of the
540 Earth's core. *Geochimica et Cosmochimica Acta*, *196*, 252-270.
541 Mann, U., Frost, D. J., & Rubie, D. C. (2009). Evidence for high-pressure core-mantle differentiation from
542 the metal–silicate partitioning of lithophile and weakly-siderophile elements. *Geochimica et*
543 *Cosmochimica Acta*, *73*(24), 7360-7386.

544 Martins, R., Kuthning, S., Coles, B. J., Kreissig, K., & Rehkämper, M. (2023). Nucleosynthetic isotope
545 anomalies of zinc in meteorites constrain the origin of Earth's volatiles. *Science*, *379*(6630), 369-
546 372.
547 Mathur, R., Mahan, B., Spencer, M., Godfrey, L., Landman, N., Garb, M., ... & Oboh-Ikuenobe, F. E.
548 (2021). Fingerprinting the Cretaceous-Paleogene boundary impact with Zn isotopes. *Nature*
549 *communications*, *12*(1), 4128.
550 McCoy-West, A. J., Fitton, J. G., Pons, M. L., Inglis, E. C., & Williams, H. M. (2018). The Fe and Zn
551 isotope composition of deep mantle source regions: Insights from Baffin Island
552 picrites. *Geochimica et Cosmochimica Acta*, *238*, 542-562.
553 McSween Jr, H. Y., Taylor, G. J., & Wyatt, M. B. (2009). Elemental composition of the Martian
554 crust. *science*, *324*(5928), 736-739.
555 McSween Jr, H. Y. (1994). What we have learned about Mars from SNC meteorites. *Meteoritics*, *29*(6),
556 757-779.
557 Miller, J., & Miller, J. C. (2018). *Statistics and chemometrics for analytical chemistry*. Pearson education.
558 Moynier, F., Vance, D., Fujii, T., & Savage, P. (2017). The isotope geochemistry of zinc and copper.
559 *Reviews in Mineralogy and Geochemistry*, *82*(1), 543-600.
560 Moynier, F., Paniello, R. C., Gounelle, M., Albarède, F., Beck, P., Podosek, F., & Zanda, B. (2011). Nature
561 of volatile depletion and genetic relationships in enstatite chondrites and aubrites inferred from Zn
562 isotopes. *Geochimica et Cosmochimica Acta*, *75*(1), 297-307.
563 Moynier, F., Beck, P., Jourdan, F., Yin, Q. Z., Reimold, U., & Koeberl, C. (2009). Isotopic fractionation of
564 zinc in tektites. *Earth and Planetary Science Letters*, *277*(3-4), 482-489.
565 Moynier, F., Albarède, F., & Herzog, G. F. (2006). Isotopic composition of zinc, copper, and iron in lunar
566 samples. *Geochimica et Cosmochimica Acta*, *70*(24), 6103-6117.
567 Nanne, J. A., Nimmo, F., Cuzzi, J. N., & Kleine, T. (2019). Origin of the non-carbonaceous–carbonaceous
568 meteorite dichotomy. *Earth and Planetary Science Letters*, *511*, 44-54.
569 Neumann, H. (1949). Notes on the mineralogy and geochemistry of zinc. *Mineralogical magazine and*
570 *journal of the Mineralogical Society*, *28*(205), 575-581.
571 Nyquist, L. E., Bogard, D. D., Shih, C. Y., Greshake, A., Stöffler, D., & Eugster, O. (2001). Ages and
572 geologic histories of Martian meteorites. In *Chronology and evolution of Mars* (pp. 105-164).
573 Springer, Dordrecht.
574 O'Neill, H. S. C., & Navrotsky, A. (1983). Simple spinels; crystallographic parameters, cation radii, lattice
575 energies, and cation distribution. *American Mineralogist*, *68*(1-2), 181-194.
576 Palme, H., & O'Neill, H. (2014). Cosmochemical Estimates of Mantle Composition. Planets, Asteriods,
577 Comets and The Solar System, Volume 2 of Treatise on Geochemistry. Edited by Andrew M.
578 Davis.
579 Paniello, R. C. (2013). *Volatization of Extraterrestrial Materials as Determined by Zinc Isotopic Analysis*.
580 Washington University in St. Louis.
581 Paniello, R. C., Day, J. M. D., & Moynier, F. (2012). Zinc isotopic evidence for the origin of the
582 Moon. *Nature*, *490*(7420), 376-379.
583 Paquet, M., Moynier, F., Yokoyama, T., Dai, W., Hu, Y., Abe, Y., ... & Yurimoto, H. (2022). Contribution
584 of Ryugu-like material to Earth's volatile inventory by Cu and Zn isotopic analysis. *Nature*
585 *Astronomy*, 1-8.
586 Paquet, M., Day, J. M., Udry, A., Hattingh, R., Kumler, B., Rahib, R. R., ... & Neal, C. R. (2021). Highly
587 siderophile elements in shergottite sulfides and the sulfur content of the Martian
588 mantle. *Geochimica et Cosmochimica Acta*, *293*, 379-398.
589 Pringle, E. A., Moynier, F., Beck, P., Paniello, R., & Hezel, D. C. (2017). The origin of volatile element
590 depletion in early solar system material: Clues from Zn isotopes in chondrules. *Earth and Planetary*
591 *Science Letters*, *468*, 62-71.
592 Rai, N., & Van Westrenen, W. (2013). Core-mantle differentiation in Mars. *Journal of Geophysical*
593 *Research: Planets*, *118*(6), 1195-1203.

Righter, K., Danielson, L. R., Pando, K., Morris, R. V., Graff, T. G., Agresti, D. G., ... & Lanzirotti, A. (2013). Redox systematics of Martian magmas with implications for magnetite stability. *American Mineralogist*, *98*(4), 616-628.

Righter, K., & Drake, M. J. (1999). Effect of water on metal-silicate partitioning of siderophile elements: a high pressure and temperature terrestrial magma ocean and core formation. *Earth and Planetary Science Letters*, *171*(3), 383-399.

Righter, K., & Drake, M. J. (1996). Core formation in Earth's moon, Mars, and Vesta. *Icarus*, *124*(2), 513-529.

Ringwood, A. E., & Hibberson, W. (1991). Solubilities of mantle oxides in molten iron at high pressures and temperatures: implications for the composition and formation of Earth's core. *Earth and Planetary Science Letters*, *102*(3-4), 235-251.

Rosman, K. J. R. (1972). A survey of the isotopic and elemental abundance of zinc. *Geochimica et Cosmochimica Acta*, *36*(7), 801-819.

Rubie, D. C., Jacobson, S. A., Morbidelli, A., O'Brien, D. P., Young, E. D., de Vries, J., ... & Frost, D. J. (2015). Accretion and differentiation of the terrestrial planets with implications for the compositions of early-formed Solar System bodies and accretion of water. *Icarus*, *248*, 89-108.

Russell, W. A., Papanastassiou, D. A., & Tombrello, T. A. (1978). Ca isotope fractionation on the Earth and other solar system materials. *Geochimica et Cosmochimica Acta*, *42*(8), 1075-1090.

Sarbadhikari, A. B., Day, J. M. D., Liu, Y., Rumble III, D., & Taylor, L. A. (2009). Petrogenesis of olivine-phyric shergottite Larkman Nunatak 06319: Implications for enriched components in Martian basalts. *Geochimica et Cosmochimica Acta*, *73*(7), 2190-2214.

Savage, P. S., Moynier, F., & Boyet, M. (2022). Zinc isotope anomalies in primitive meteorites identify the outer solar system as an important source of Earth's volatile inventory. *Icarus*, 115172.

Schiller, M., Bizzarro, M., & Siebert, J. (2020). Iron isotope evidence for very rapid accretion and differentiation of the proto-Earth. *Science advances*, *6*(7), eaay7604.

Schiller, M., Bizzarro, M., & Fernandes, V. A. (2018). Isotopic evolution of the protoplanetary disk and the building blocks of Earth and the Moon. *Nature*, *555*(7697), 507-510.

Sossi, P. A., Stotz, I. L., Jacobson, S. A., Morbidelli, A., & O'Neill, H. S. C. (2022). Stochastic accretion of the Earth. *Nature Astronomy*, *6*(8), 951-960.

Sossi, P. A., Nebel, O., O'Neill, H. S. C., & Moynier, F. (2018). Zinc isotope composition of the Earth and its behaviour during planetary accretion. *Chemical Geology*, *477*, 73-84.

Sossi, P. A., Halverson, G. P., Nebel, O., & Eggins, S. M. (2015). Combined separation of Cu, Fe and Zn from rock matrices and improved analytical protocols for stable isotope determination. *Geostandards and Geoanalytical Research*, *39*(2), 129-149.

Steenstra, E. S., & van Westrenen, W. (2018). A synthesis of geochemical constraints on the inventory of light elements in the core of Mars. *Icarus*, *315*, 69-78.

Steller, T., Burkhardt, C., Yang, C., & Kleine, T. (2022). Nucleosynthetic zinc isotope anomalies reveal a dual origin of terrestrial volatiles. *Icarus*, 115171.

Symes, S. J., Borg, L. E., Shearer, C. K., & Irving, A. J. (2008). The age of the Martian meteorite Northwest Africa 1195 and the differentiation history of the shergottites. *Geochimica et Cosmochimica Acta*, *72*(6), 1696-1710.

Tait, K. T., & Day, J. M. D. (2018). Chondritic late accretion to Mars and the nature of shergottite reservoirs. *Earth and Planetary Science Letters*, *494*, 99-108.

Taylor, G. J. (2013). The bulk composition of Mars. *Geochemistry*, *73*(4), 401-420.

Taylor, G. J., Boynton, W., Brückner, J., Wänke, H., Dreibus, G., Kerry, K., ... & Drake, D. (2006). Bulk composition and early differentiation of Mars. *Journal of Geophysical Research: Planets*, *111*(E3).

Thomas-Keprta, K. L., Clemett, S. J., Mckay, D. S., Gibson, E. K., & Wentworth, S. J. (2009). Origins of magnetite nanocrystals in Martian meteorite ALH84001. *Geochimica et Cosmochimica Acta*, *73*(21), 6631-6677.

643 Tian, Z., Magna, T., Day, J. M. D., Mezger, K., Scherer, E. E., Lodders, K., ... & Wang, K. (2021).
644 Potassium isotope composition of Mars reveals a mechanism of planetary volatile
645 retention. *Proceedings of the National Academy of Sciences*, *118*(39), e2101155118.
646 Toutain, J. P., Sonke, J., Munoz, M., Nonell, A., Polvé, M., Viers, J., ... & Sumarti, S. (2008). Evidence for
647 Zn isotopic fractionation at Merapi volcano. *Chemical Geology*, *253*(1-2), 74-82.
648 Treiman, A. H. (2005). The nakhlite meteorites: Augite-rich igneous rocks from
649 Mars. *Geochemistry*, *65*(3), 203-270.
650 Treiman, A. H., Gleason, J. D., & Bogard, D. D. (2000). The SNC meteorites are from Mars. *Planetary and*
651 *Space Science*, *48*(12-14), 1213-1230.
652 Trinquier, A., Elliott, T., Ulfbeck, D., Coath, C., Krot, A. N., & Bizzarro, M. (2009). Origin of
653 nucleosynthetic isotope heterogeneity in the solar protoplanetary disk. *Science*, *324*(5925), 374-
654 376.
655 Trinquier, A., Birck, J. L., & Allègre, C. J. (2007). Widespread ^{54}Cr heterogeneity in the inner solar
656 system. *The Astrophysical Journal*, *655*(2), 1179.
657 Udry, A., Howarth, G. H., Herd, C. D. K., Day, J. M. D., Lapen, T. J., & Filiberto, J. (2020). What Martian
658 meteorites reveal about the interior and surface of Mars. *Journal of Geophysical Research: Planets,*
659 *125*, 1-34.
660 Udry, A., & Day, J. M. D. (2018). 1.34 billion-year-old magmatism on Mars evaluated from the co-genetic
661 nakhlite and chassignite meteorites. *Geochimica et Cosmochimica Acta*, *238*, 292-315.
662 van Kooten, E., & Moynier, F. (2019). Zinc isotope analyses of singularly small samples (< 5 ng Zn):
663 investigating chondrule-matrix complementarity in Leoville. *Geochimica et Cosmochimica*
664 *Acta*, *261*, 248-268
665 Wadhwa, M. (2001). Redox state of Mars' upper mantle and crust from Eu anomalies in shergottite
666 pyroxenes. *Science*, *291*(5508), 1527-1530.
667 Wang, Z., Laurenz, V., Petitgirard, S., & Becker, H. (2016). Earth's moderately volatile element
668 composition may not be chondritic: Evidence from In, Cd and Zn. *Earth and Planetary Science*
669 *Letters*, *435*, 136-146.
670 Warren, P. H. (2011). Stable-isotopic anomalies and the accretionary assemblage of the Earth and Mars: A
671 subordinate role for carbonaceous chondrites. *Earth and Planetary Science Letters*, *311*(1-2), 93-
672 100.
673 Wetherill, G. W. (1994). Provenance of the terrestrial planets. *Geochimica et Cosmochimica Acta*, *58*(20),
674 4513-4520.
675 Wood, B. J., Smythe, D. J., & Harrison, T. (2019). The condensation temperatures of the elements: A
676 reappraisal. *American Mineralogist: Journal of Earth and Planetary Materials*, *104*(6), 844-856.
677 Wood, B. J., Kiseeva, E. S., & Mirolo, F. J. (2014). Accretion and core formation: The effects of sulfur on
678 metal–silicate partition coefficients. *Geochimica et Cosmochimica Acta*, *145*, 248-267.
679 Xia, Y., Kiseeva, E. S., Wade, J., & Huang, F. (2019). The effect of core segregation on the Cu and Zn
680 isotope composition of the silicate Moon. *Geochemical Perspectives Letters*, *12*, 12-17.
681 Yoshizaki, T., & McDonough, W. F. (2020). The composition of Mars. *Geochimica et Cosmochimica*
682 *Acta*, *273*, 137-162.
683
684

685 **Table captions**

686 Table 1. Zinc stable isotope and major element compositions of Martian meteorites.

687 Table 2. Mixing models.

688

689 **Figures and figure captions**

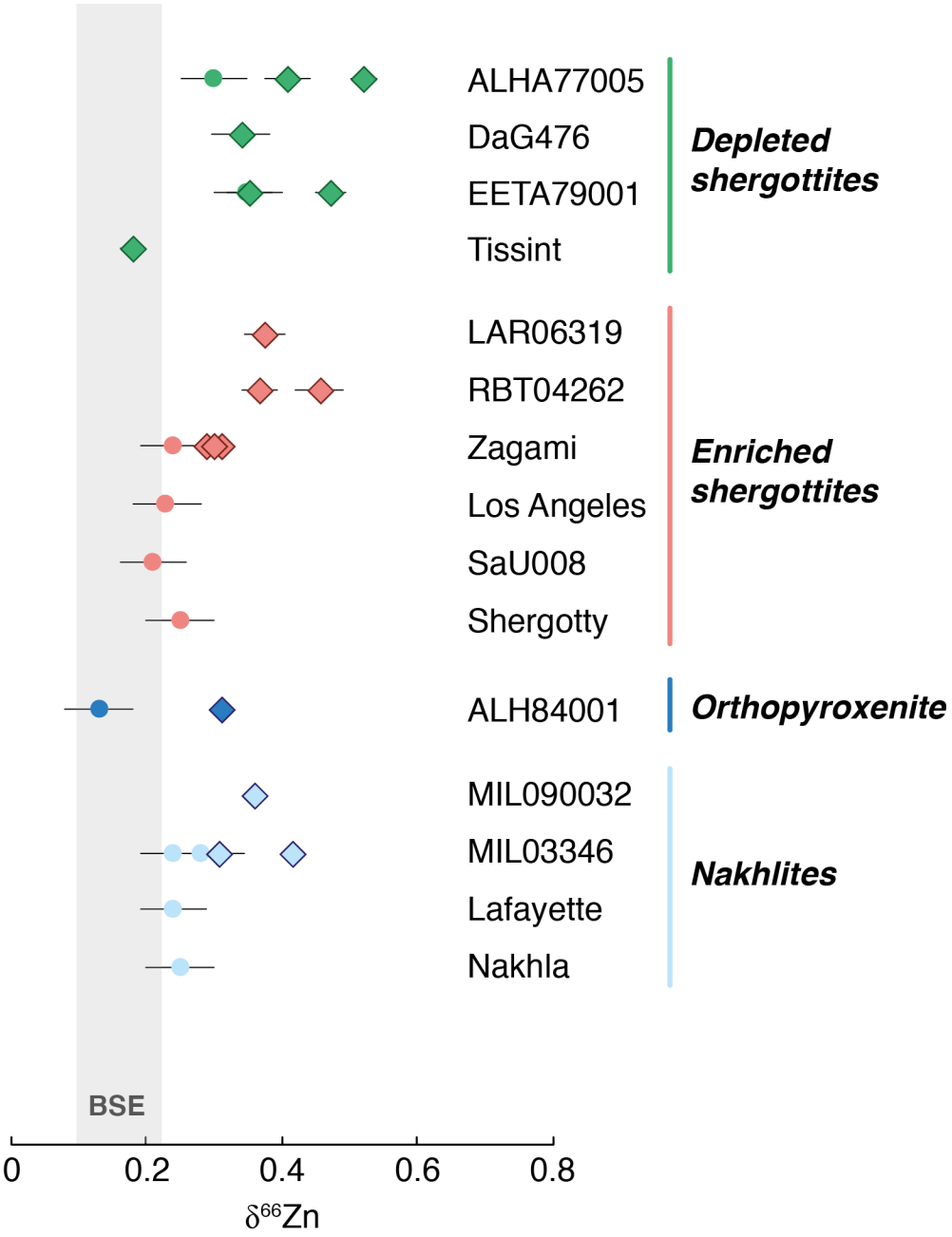

690

691 ***Figure 1.*** *Zinc isotope composition for all Martian samples. Bulk Silicate Earth (BSE – gray*
692 *field) from Sossi et al. (2018). Diamonds: this study; circles: Paniello et al., (2012). Error bars:*
693 *2SD.*

694

695

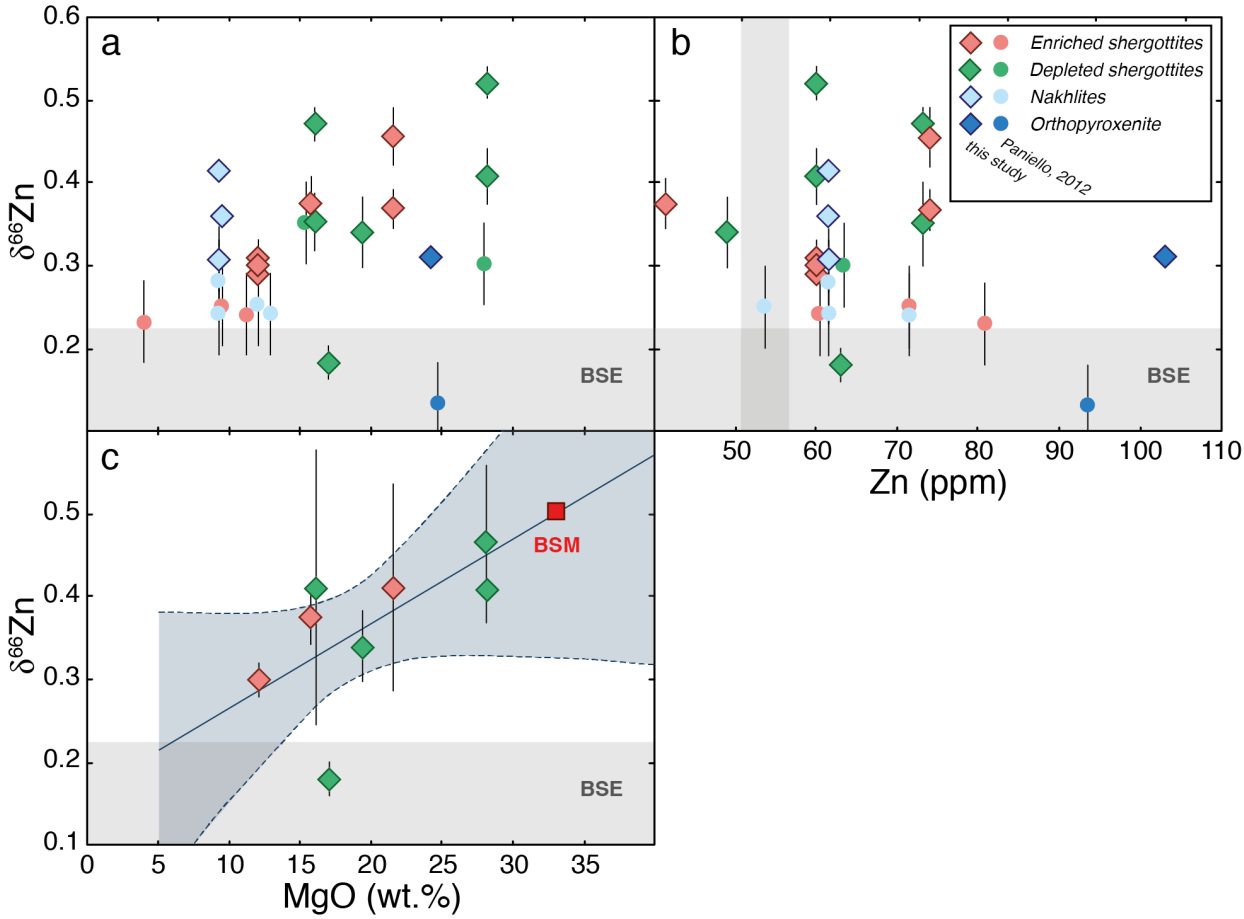

Figure 2. *δ^{66}Zn as a function of the (a) MgO content (wt.%) and (b) Zn content (ppm) for all Martian meteorites (diamonds: this study). (c) Average δ^{66}Zn for each Martian meteorite as a function of the MgO content (wt.%) for the shergottites from this study. Literature data (circles) are from Paniello et al. (2012) for Zn isotopes and elemental compositions; MgO content from Tait and Day, 2018). Bulk Silicate Earth composition range for δ^{66}Zn (gray field) from Sossi et al. (2018). The solid line in (c) is the linear regression of the dataset (R^2=0.65 excluding Tissint), and the dashed lines represent the 95% confidence error envelope. BSM is the Bulk Silicate Mars estimate. Error bars: 2SD.*

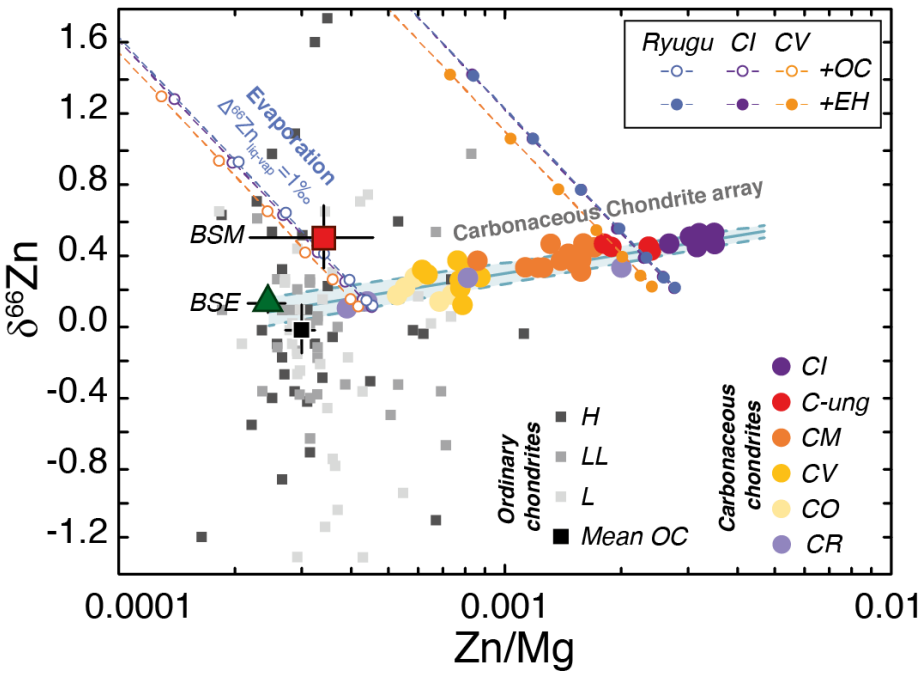

Figure 3. *Zinc isotope compositions of planetary materials (modified from Sossi et al. (2018)). Literature data for the Zn isotope and elemental compositions from: carbonaceous chondrites (Luck et al., 2005; Pringle et al., 2017; Mahan et al.,2018; Paquet et al., 2022), CR (Mahan et al., 2018) and ordinary chondrites (Paniello, 2013, PhD thesis Washington University Saint Louis; Creech and Moynier, 2019); see SourceData table for Mg contents. Bulk Silicate Earth composition from Palme and O'Neill (2014) and Sossi et al., (2018); carbonaceous chondrite array from Sossi et al. (2018). The dashed lines represent the fraction of Zn evaporated from a starting composition deriving from mixing between carbonaceous (4 % Ryugu-like material, 6 % CI or 14 % CV) and non-carbonaceous materials (96 %, 94 % or 86 %, respectively) (fractionation factor of* $\Delta^{66}Zn_{liq\text{-}vap}$ *= +1 ‰, with a 5% increment step (see Table 2 and text for details)). The Bulk Silicate Mars plots away from the carbonaceous chondrite array. The error for the BSM estimate represents the 95 % confidence interval for MgO =32.8 wt.% (Khan et al., 2022) derived from the linear regression in Figure 2c.*

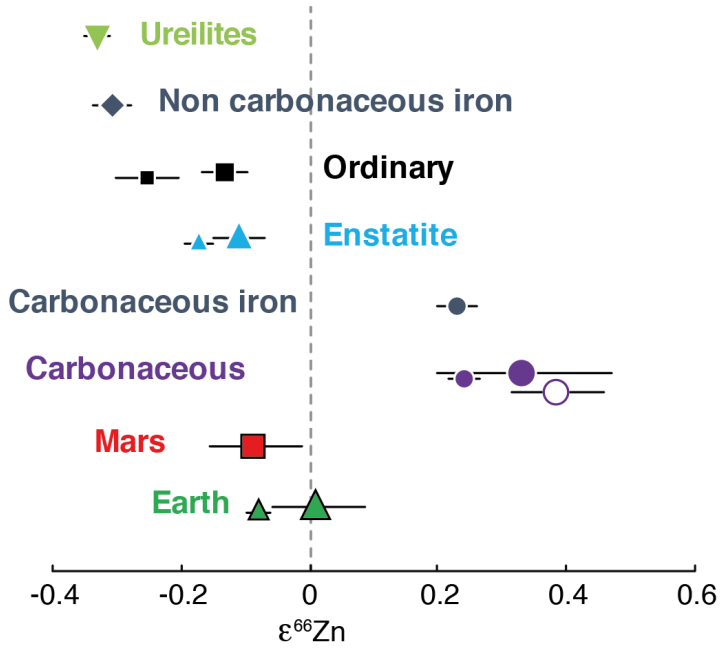

Figure 4. *Variations of $\varepsilon^{66}Zn$ among different groups of meteorites, Mars (this study) and the Earth. Literature data for carbonaceous chondrites (Savage et al., 2022 (large symbols); Steller et al., 2022 (small symbols); Paquet et al., 2022 (open circle)), ordinary and enstatite chondrites, carbonaceous and non-carbonaceous iron meteorites and ureilites (Savage et al., 2022; Steller et al., 2022). Bulk Silicate Earth value for $\varepsilon^{66}Zn$ is +0.015 ± 0.075 (2SE; Savage et al., 2022) and –* 0.07 ± 0.013 *(2SE; Steller et al., 2022). Error bars are 2SE.*

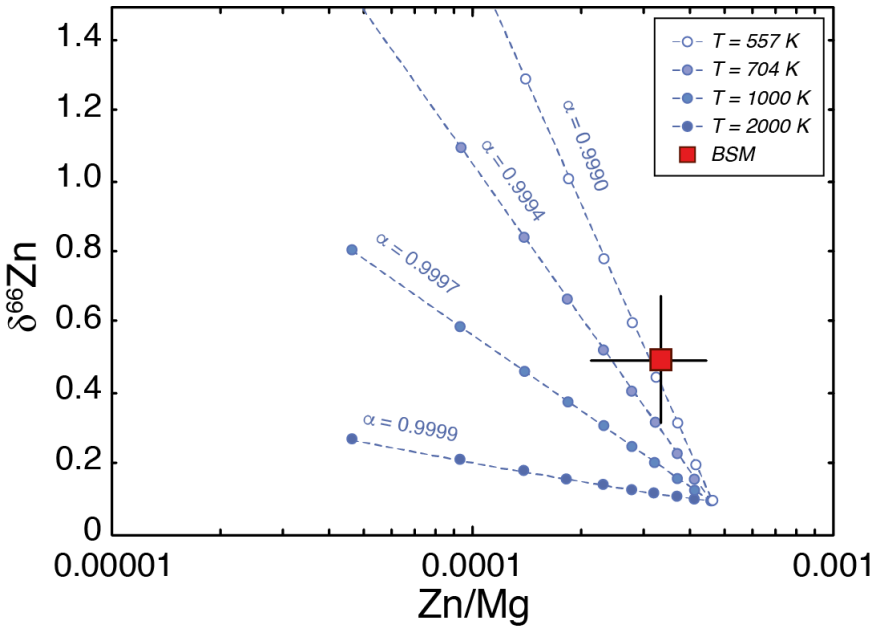

731

732 ***Figure 5.*** *Equilibrium evaporation trajectories for different isotope fractionation factors α,*
733 *which depend on the temperature T (in K). The starting point for the models was based upon the*
734 *assumption that the original building blocks of Mars had 96 % OC and 4 % Ryugu-like material*
735 *contribution.*

736 **Supplementary figures and figure captions**

737

738

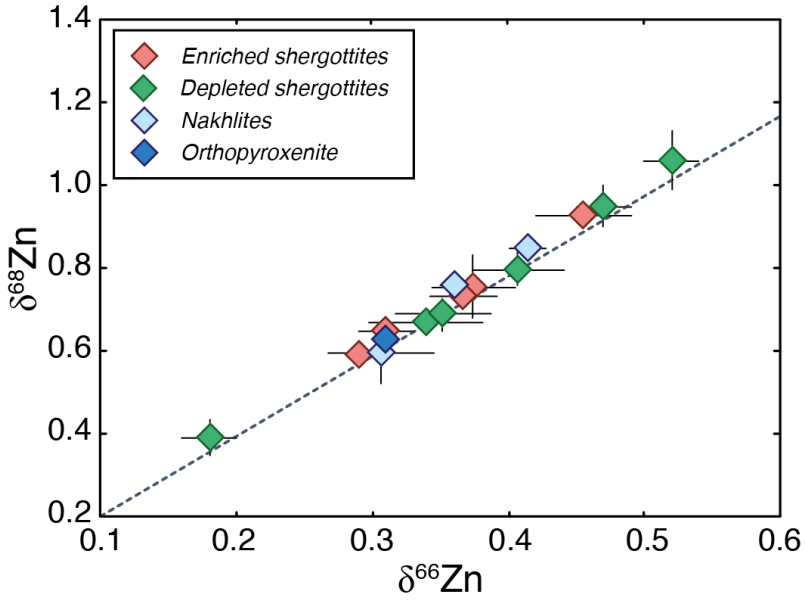

739

740 ***Figure S1.*** *δ^{68}Zn versus δ^{66}Zn for Martian meteorites. All samples fall slightly above the mass-*

741 *dependent fractionation line. Analytical errors (2SD) are reported. Green: depleted shergottites;*

742 *red: enriched shergottites; light blue: nakhlites; dark blue: orthopyroxenite.*

743